LENGTH- AND AGE-AT-SPAWNING OF ANTARCTIC TOOTHFISH (*DISSOSTICHUS MAWSONI*) IN THE ROSS SEA

S.J. Parker✉
National Institute of Water and
Atmospheric Research (NIWA) Ltd
PO Box 893
Nelson, New Zealand
Email – s.parker@niwa.co.nz

P.J. Grimes
NIWA Ltd
Private Bag 14901
Wellington, New Zealand

Abstract

This study uses histological assessments to determine age- and length-at-spawning for female and male Antarctic toothfish (*Dissostichus mawsoni*) from fish sampled in the Ross Sea spanning the 2000–2009 fishing seasons. A characterisation of the oocyte developmental cycle of *D. mawsoni* shows that once development begins, oocytes grow and accumulate at the cortical alveoli stage for at least one year. Individual oocytes are then recruited into the vitellogenic phase over at least a 6–12 month period, resulting in a developed group of oocytes accumulating at the final maturation stage by approximately May each year. The age at 50% spawning for females on the Ross Sea slope region is 16.6 years (95% CI 16.0–17.3) or 133.2 cm (95% CI 130.9–135.7) by length. On average, males spawn at a younger age with an $A_{50\%}$ of 12.8 years (95% CI 11.9–14.0) or 120.4 cm (95% CI 114.8–126.7) by length. Evidence of skip-spawning was observed for females only and results in a flatter, right-shifted ogive, increasing the functional difference between male and female ogives. The degree to which the overall population ogive is biased right (older) by applying the slope-derived ogive to the northern Ross Sea region depends on the proportion of the total population occurring in the northern Ross Sea region, which is currently unknown.

Résumé

Cette étude utilise des évaluations histologiques pour déterminer l'âge et la longueur à la première reproduction des légines antarctiques (*Dissostichus mawsoni*) mâles et femelles échantillonnées en mer de Ross pendant les saisons de pêche 2000–2009. Une caractérisation du cycle de développement des ovocytes de *D. mawsoni* indique qu'une fois commencé le processus, les ovocytes se développent et s'accumulent au stade des alvéoles corticaux pendant au moins un an. Les ovocytes sont alors recrutés individuellement dans la phase de vitellogénèse au cours d'une période d'au moins 6–12 mois, avec pour résultat une accumulation d'ovocytes ayant atteint le stade de maturité vers mai chaque année. L'âge auquel 50% des femelles se reproduisent dans la région de la pente de la mer de Ross est de 16,6 ans (intervalle de confiance à 95% (IC) 16,0–17,3), ce qui correspond à 133,2 cm de longueur (IC à 95% 130,9–135,7). En moyenne, l'âge du frai est moins élevé chez les mâles : $A_{50\%}$ est de 12,8 ans (IC à 95% 11,9–14,0) ou 120,4 cm de longueur (IC à 95% 114,8–126,7). Des observations mettent en évidence que les femelles ne se reproduisent pas tous les ans ; l'ogive en résultant est de forme plus aplatie et est déplacée vers la droite, ce qui augmente la différence fonctionnelle des ogives entre les mâles et les femelles. Le degré auquel l'ogive de l'ensemble de la population est biaisée vers le côté droit (plus âgé) lorsque l'ogive dérivée de la pente est appliquée à la mer de Ross dépend de la proportion de l'ensemble de la population présente dans la région du nord de la mer de Ross, ce qui est actuellement inconnu.

Резюме

В данном исследовании используются гистологические оценки для определения возраста и длины при нересте самок и самцов антарктического клыкача (*Dissostichus mawsoni*) по образцам рыбы, полученной в море Росса в период, охватывающий промысловые сезоны 2000–2009 гг. Описание цикла развития ооцитов у *D. mawsoni* показывает, что, как только начинается развитие, ооциты растут и аккумулируются на стадии кортикальных альвеол на протяжении по крайней мере одного года.

Отдельные ооциты затем в течение по крайней мере 6–12 месяцев переходят в вителлогенную фазу, в результате чего на окончательной стадии созревания ежегодно приблизительно к маю накапливается развитая группа ооцитов. В районе склона моря Росса в 50% случаев возраст самок при нересте составляет 16.6 лет (95% ДИ 16.0–17.3), а длина – 133.2 см (95% ДИ 130.9–135.7). Самцы в среднем нерестятся в более раннем возрасте при $A_{50\%}$ 12.8 лет (95% ДИ 11.9–14.0) или длине 120.4 см (95% ДИ 114.8–126.7). Случаи пропусков нереста наблюдались только у самок, что вело к более плоской сдвинутой вправо огиве, усугубляя функциональные различия между огивами самцов и самок. Степень, в которой огива всей популяции смещена вправо (старший возраст) при применении полученной для склона огивы к северной части региона моря Росса, зависит от того, какая доля общей популяции встречается в северной части региона моря Росса, что в настоящее время неизвестно.

Resumen

Este estudio se vale de exámenes histológicos para determinar la edad y talla de desove y espermiación de hembras y machos de austromerluza negra (*Dissostichus mawsoni*) capturados en el Mar de Ross en las temporadas de pesca de 2000–2009. Una caracterización del ciclo de desarrollo de los ovocitos de *D. mawsoni* muestra que, una vez que comienza la formación de ovocitos, éstos crecen y se acumulan en la fase de alvéolo cortical por un año por lo menos. Luego cada ovocito pasa a la fase vitelogénica durante un período de 6–12 meses por lo menos, formando un grupo de ovocitos desarrollados al final de la etapa de maduración alrededor de mayo de cada año. La edad de desove para el 50% de las hembras en la región del talud del Mar de Ross es de 16.6 años (16.0–17.3 IC de 95%) o 133.2 cm de longitud (130.9–135.7 IC de 95%). En general la espermiación en los machos ocurre más temprano, siendo $A_{50\%}$ 12.8 años (11.9–14.0 IC de 95%) o 120.4 cm de longitud (114.8–126.7 IC de 95%). Se observaron signos en hembras solamente de que el desove a veces no ocurre, lo que resulta en una ojiva más plana desplazada hacia la derecha, aumentando la diferencia funcional entre las ojivas de los machos y de las hembras. El grado de desviación hacia la derecha (de más edad) de la ojiva de la población total que resulta al aplicar la ojiva derivada del talud a la región norte del Mar de Ross, depende de la proporción de la población total que habita en la región norte del Mar de Ross, que por ahora se desconoce.

Keywords: maturity, oogenesis, skip-spawning, ogive, CCAMLR

Introduction

The reproductive ecology of Antarctic toothfish (*Dissostichus mawsoni*) in the Ross Sea has been difficult to resolve because the spatial dynamics of the stock, and logistical constraints on access to fish have prevented collecting appropriate spatially, and temporally distributed samples (Dunn and Hanchet, 2007; Hanchet et al., 2008). Existing macroscopic staging data, gonadosomatic index (GSI) analysis, and histological forecasting studies have not been comprehensive and have not been synthesised with the known biological characteristics of notothenioids to characterise reproduction in this species. This paper provides additional histological data and a species-specific characterisation of oogenesis to more robustly estimate length- and age-at-spawning for stock assessment purposes.

In notothenioid females, evaluating developmental status is complicated by a prolonged oogenesis in which oocyte development is at least a two-year process, although spawning may then take place annually (Everson, 1970; Sil'yanova, 1982; Everson, 1984; Kock and Kellermann, 1991; Shandikov and Faleeva, 1992). This results in multiple size modes of developing oocytes present in the ovary throughout the year, making macroscopic staging inadequate to describe patterns of development. Additional evidence from other notothenioid species shows that oocytes grow slowly to the cortical alveoli stage (endogenous yolk) and accumulate prior to entering exogenous vitellogenesis (α-stage oocytes of Everson, 1970, 1994). Protracted oocyte growth may be necessary to produce the relatively large, yolky eggs (>4.0 mm) observed in this group. Prolonged oogenesis has been mentioned in several studies on reproduction in *D. mawsoni*, though the details of cellular development have not been described (Eastman and DeVries, 2000; Livingston and Grimes, 2005; Piyanova and Petrov, 2007). This reproductive characteristic has been documented in other cold-water species (Junquera et al., 2003; Alekseyeva et al., 1993).

Histological assessment of reproductive status directly observes the physiological status of gametes and, given an appropriate sampling design (sample size and spatio–temporal distribution), an accurate assessment is possible. Samples in the

Ross Sea are typically available only from the summer months (December to February) during the commercial fishery, far removed from the likely spawning period between June and September. Without collecting samples just prior to, or during, the winter spawning season, the best method available to assess spawning status is to seek histological evidence of spawning in the ovaries of fish sampled after the spawning season (hindcasting). This evidence consists of post-ovulatory follicles (POFs), residual eggs, atretic oocytes of an advanced stage, as well as other supporting evidence such as ovarian wall thickness, oocyte packing density and degree of ovarian vascularisation (Murua et al., 2003; Livingston and Grimes, 2005; Burton et al., 1997). Some of these characters may be modified or resorbed as new development begins, but others may last several months to a year, tending to persist the longest in cold-water species (Everson, 1970; Shandikov and Faleeva, 1992; Junquera et al., 2003; Saborido-Rey and Junquera, 1998; Rideout et al., 2005).

Length-at-spawning for *D. mawsoni* males has also been estimated from macroscopic staging data, GSI analysis and histological studies (Patchell, 1999; Patchell, 2001; Hanchet and Horn, 2000). Male notothenioids typically have a one-year gamete development cycle and testis size increases dramatically late in the summer to autumn with most fish in a resting stage during the summer (Kock and Kellermann, 1991; Fenaughty, 2006; Piyanova, 2008). A histologically based assessment of male age-at-spawning can extend the period in which development can be detected by examining development at the cellular level within the testes.

The primary objective of this study is to use extensive gonad sample collections for histological evaluation to generate length- and age-at-spawning relationships for *D. mawsoni* in the Ross Sea for use in stock assessments. To aid in interpretation of the histology and describe the developmental process, oogenesis is described and available information on the size and growth rates of oocyte classes is summarised. Finally, histological assessment of males is also conducted to develop length- and age-at-spawning relationships for use in stock assessments.

Methods

Ovary and testis samples from *D. mawsoni* were collected by scientific observers on board commercial fishing vessels. In general, samples were only available between December and February in each year, though some late-season samples were available in 2000–2002 because the fishery lasted longer. In addition, samples were collected only where the fishery occurred, which meant fewer samples were collected in the northern and shelf regions, and samples were concentrated along the continental slope, following the distribution of catch limits. Hanchet et al. (2008) hypothesise that juvenile toothfish occur mainly on the shelf, with adults congregating on the slope and migrating to northern areas to spawn, so the analysis presented here addresses each region separately. A limited number of samples from later in the season were used to describe the time course of oogenesis.

Gonad samples were fixed in 10% buffered formalin, processed as 5 µm sections in paraffin, stained with Haematoxylin and Eosin Y or Periodic acid-Schiff (PAS) and viewed with a stereo microscope at x10–x400 magnification. Along with tissue samples, information such as length, weight, sex, gonad weight, macroscopic stage, sampling location and depth was also collected.

For each histological sample, any evidence of previous spawning activity, such as POFs, significant atresia, or residual eggs was recorded. Also measured were the thickness of the ovarian wall, and qualitatively scored oocyte packing density, lamellar packing, and degree of vascularisation present as support for the evaluation. The most advanced developmental stage in each histological section was recorded along with the mean maximum viable oocyte diameter (mean of five largest oocytes (West, 1990)).

Spawning status in the previous winter was assigned based on the presence of POFs, significant levels of atresia of advanced stages, or residual eggs. Hindcasting does not utilise the most advanced developmental status of viable oocytes. However, an analysis was conducted to confirm that POFs were indeed detectable throughout the period sampled (see below). For comparative purposes, the forecasting method was also conducted and spawning status in the upcoming season was assigned based on the most advanced viable oocyte stage in each sample. Following Everson (1970) and Kock and Kellermann (1991), samples with the most advanced oocyte stage of cortical alveoli (end of the primary growth phase) were classified as 'not spawned'.

Ages were determined following Horn (2002) for all sampled individuals using otoliths. Because sampling occurs so far from the spawning season, the size and age of the fish would be different during the actual spawning season. Ages are incremented on 1 July, so a fish that turned 10 on 1 July is recorded as 10 when sampled in the subsequent

Table 1: Temporal and spatial distribution of *Dissostichus mawsoni* ovary samples collected by scientific observers in the Ross Sea longline fisheries. Note, only December to March samples from the slope region were used to determine the female proportion spawning ogive. Samples from other periods and locations were used to describe the developmental cycle.

Month	Fishing year	North	Slope	Shelf	Subarea 88.2	SSRU 5842E	Total
December	2004	1					1
	2006	70	40	12			122
	2007	59	3				62
	2009	64					64
January	2001			8			8
	2004		70	17			87
	2006		131				131
	2007		250				250
	2009		92	12			104
February	2002		12	8			20
	2006	4	6				10
	2007		21				21
	2009				37		37
March	2000		46				46
	2001	2	57				59
	2002		56				56
	2005					69	69
April	2001	2	1				3
May	2001	15					15
Total		217	785	57	37	69	1165

summer fishery. The age-at-spawning for the forecasting method is then one year older than the age used for the hindcasting method, and size is accordingly different. To compare the forecasting and hindcasting methods, fish ages for the forecasting method were advanced one year. Fish lengths for either method were adjusted using the sample date, and adjusted down or up using the von Bertalanffy growth relation from Hanchet (2006).

The proportion spawning P_s was modelled as a function of length (L) or age (A) using a binomial distribution with logit link:

$$P_s = \alpha + \beta * L \text{ or } A$$
$$L_{50\%} \text{ or } A_{50\%} = -(\alpha / \beta).$$

Results

Samples collected

A total of 1 165 ovary samples was collected by observers during the fishing years 2000–2009, with 1 059 available within Subarea 88.1 of the Ross Sea (Table 1). Most samples were collected between mid-December and early-February with a spatial coverage of the shelf, slope and northern regions of the Ross Sea. Histological samples from 59 males were also collected in 2009 or 2001 from the north, slope and shelf regions. Within the Ross Sea, sample distribution was concentrated along the continental slope in SSRUs 881H and 881I, fishable depths of SSRU 881C in the northern region and Terra Nova Bay (SSRU 881M) (Figure 1).

Histological assessment

Oogenesis

Samples of spawning fish between December and February show oocytes in the secondary or exogenous growth phase, termed vitellogenesis, developing to be spawned in the upcoming season (Figures 2b and d). Throughout the developmental period, large fish were more advanced than smaller fish (Figure 3a). Early vitellogenic (EVG) stage oocytes are typically 600–750 µm in diameter and late vitellogenic (LVG) stage oocytes are typically 750–1 200 µm (Figure 3b). In addition to the large vitellogenic oocytes, a second class of oocytes undergoing primary (or endogenous) growth is present with cell diameters typically ranging from 300–600 µm, and diagnosed by the large number of clear cytoplasmic vacuoles (cortical alveoli (CA)) surrounding the nucleus (Figures 2a, 2b and 2d). A class of still smaller, basophilic oocytes (typically darker staining with nucleoli) at the late perinucleolus (LPN) stage ranging in size from 200–300 µm

is always present, and is the maximum oocyte size observed in immature females. Early perinucleolus oocytes (EPN), diagnosed by dark staining cytoplasm and a large uniform nucleus, or the even smaller oogonium phase (OOG), are often visible but may not be abundant in a recently spawned ovary. These cells range in size from 20–150 μm.

Later in the season, some larger fish reach the germinal vesicle migration (GVM) stage (1 500–2 500 μm), or even the maturing oocyte stage (MAT), characterised by the breakdown of the nucleus and coalescence of the yolk granules into a large homogenous yolk droplet (Figures 2b and 2d).

In a female developing to spawn in the upcoming season, cells are recruited from the CA stage into the vitellogenic stage and then increase in size as yolk deposition occurs during the summer months (Figure 3 b). The cell diameters for CA-stage oocytes do not grow much in excess of 500–600 μm before transforming to EVG cells (Figure 3b). By March, the EVG recruitment process ceases and existing vitellogenic oocytes grow and accumulate at the GVM stage producing a distinct size mode at 1 500–1 800 μm (Figure 4). This process results in maturing ovaries with large GVM-stage cells, plus CA, LPN and EPN visible in the lamellae (Figure 2d). No samples had LVG-stage cells without also having CA-stage cells, indicating that although development from the LPN stage takes two years, a continuous supply of CA-stage cells means spawning could occur every year. For toothfish, consistent with other notothenioids, individuals with only CA-stage cells are still immature. The GVM cells determine the potential batch size to be spawned in the upcoming season, characterising *D. mawsoni* as a determinate group synchronous spawning species, with a hiatus in development not between LPN- and CA-stage cells, but between CA stage and EVG cells. The overall pattern, seasonality and developmental timing of oogenesis in *D. mawsoni* is depicted in Figure 5.

Evidence of previous spawning

Evidence of spawning during the previous season was established based on the presence of POFs or residual oocytes arrested at the GVM, prematuration, or mature stage of development. These oocyte remnants were observed within the matrix of other developing cells. POFs were distinguishable in histological samples from December to April, and often co-occurred with atretic cells still identifiable as GVM stage (Figures 2d, 2e and 2f).

The proportion of fish at a given size with detectable POFs in each month showed no overall trend with time, indicating that during the December to February period, POFs remained detectable in the ovaries (Figure 6). The few existing samples from May indicated resorption was accelerating and POFs, though still present at some level, were smaller and more difficult to detect. To avoid bias from the decrease in detectability as POFs were resorbed, only samples from December to February were used for hindcasting spawning status. In contrast, forecasting methods included samples through to May where available.

Skip spawning

Evidence for skipped spawning was also present in *D. mawsoni* females. Fish with developing LVG and no evidence of previous spawning were either preparing to spawn for the first time, have not spawned for at least a year, or all remnants of spawning had been resorbed. Almost 50% of CA-stage or 40% of EVG-stage fish on the slope showed no indication of spawning in the previous season, indicating they had either skipped spawning in the previous year or were developing to spawn for the first time (Table 2). Of the EVG-stage fish that did not spawn in the previous season, 70% were between 13 and 18 years old, suggesting that skip-spawning may be primarily an adolescent feature, though 17% were over 18 years old. Although large or old 'not-spawned' fish were observed, they were not common. Very few fish in the northern area were classified as not spawned (Table 2). Ovary wall thickness on these few specimens was typically >1 000 μm, indicating they had spawned at some time in the past. Most of the fish from shelf samples were classified as not spawned, and only 10 of 40 fish there showed evidence of spawning six months earlier. All these fish were from areas close to the slope. The small sample size from the shelf area prevents an analysis of potential skip-spawning by age.

Length- and age-at-spawning

Females

Once spawning status was described for each fish, the proportion spawning by age or length was fitted with a logistic model. Several spawning assessment methods were compared using the slope data, where sample sizes were the highest. Hindcasting with all data and with forecasting data showed similar relationships with age and length (Table 3; Figure 7). The age at 50% spawning for females on the Ross Sea slope region is 16.6 years (95% CI 16.0–17.3) or 133.2 cm (95% CI 130.9–135.7) by length. The main difference between the hindcasting and forecasting methodologies was a small

Table 2: Summary of developmental status based on histological assessment of *Dissostichus mawsoni* ovaries collected during the summer fishing months in the Ross Sea, 2004–2009. Values are numbers of fish. EPN – early perinucleolus, LPN – late perinucleolus, CA – cortical alveoli, EVG – early vitellogenesis, LVG – late vitellogenesis, GVM – germinal vesicle migration, MAT – maturing.

Most advanced histological stage	North		Slope		Shelf		Total
	Not spawned	Spawned	Not spawned	Spawned	Not spawned	Spawned	
EPN			114		3		117
LPN	1		188		21		210
CA	3		62	56	12	1	134
EVG		1	38	50	2	5	96
LVG		182	4	87		1	276
GVM		4		1		3	6
MAT		5					5
Total	4	192	406	194	38	10	844

Table 3: Details of the length- or age-at-spawning ogive fits for *Dissostichus mawsoni* from the Ross Sea using hindcasting or forecasting methodologies. $L_{95\%}$ or $A_{95\%}$ indicate the length or age to be added to the $L_{50\%}$ value to reach the 95th percentile.

Region	Sex	Method	*N*	$L_{50\%}$ or $A_{50\%}$	$L_{95\%}$ or $A_{95\%}$	95% CI
Slope	Female	Hindcast				
		Length	599	133.2	29.9	130.9–135.7
		Age		16.6	7.3	16.0–17.3
		Forecast				
		Length	762	136.4	20.7	134.8–138.1
		Age		17.2	6.7	16.7–17.7
All	Male	Length	56	120.4	19.7	114.8–126.7
		Age		12.8	3.5	11.9–14.0

decrease in proportion spawning for adolescent fish, suggesting that the hindcasting method detected previous spawning of individuals that typically would not have developed enough to be considered spawning using the forecasting method.

Evidence of skipped spawning is apparent in the lack of a steep ogive, as 100% of the older or larger fish do not spawn in a given year (Figure 7). It is not possible with current techniques to distinguish skipped spawning from first-time spawning in adolescent females.

Sample size for fish in the north was more limited, especially for smaller fish. To further compare spawning in the slope and north areas, the ogive generated from the slope was applied to the slope age-frequency distribution (data from Dunn and Hanchet, 2009), resulting in an age-frequency distribution for spawning fish. This was plotted along with the mean age-frequency distribution of the northern population derived from the stock assessment model (Figure 8). Spawning females on the slope were slightly younger than northern females, suggesting that adolescent fish on the slope do not initially migrate to the northern spawning grounds to spawn. If they do, they return to the slope quickly as they are not captured there during the summer fishery. In addition, as only four of 196 females sampled in the north were assessed as not spawned, it is likely that all the fish inhabiting the northern region spawned in the previous season (Table 2).

Males

Histological preparations of testis samples were evaluated for the presence of developing spermatocytes. Testes were found to be in one of three stages:

Immature – containing only spermatogonia or spermatocytes (Figure 9a)

Developing – containing spermatids (Figure 9b)

Spawning – containing spermatozoa filling lobules within the testis duct system (Figure 9c).

Individuals with either developing or spawning characteristics were classified as spawning. Ogives fit to these data yielded steep relationships with both age and length (Table 3; Figure 10). On average, males spawn at a younger age than females, with an $A_{50\%}$ of 12.8 years (95% CI 11.9–14.0) or 120.4 cm (95% CI 114.8–126.7) by length. However, because of a small sample size, the analysis pooled samples from the north (n = 21), slope (n = 20) and shelf (n = 15) regions. As the male analysis used a forecasting method, age is one year older at spawning and length values were projected forward to 1 July using the growth curve. Therefore, the male ogive is comparable with the female forecasting ogive. The steepness of the male ogive suggests that skip-spawning is not likely to occur.

Discussion

The 2007 stock assessment for *D. mawsoni* assumed an $A_{50\%}$ of 9 years, corresponding to an $L_{50\%}$ of 100 cm (95% range of ±15 cm), but noted that the parameters were uncertain and that the transition to maturity may occur at larger sizes (Hanchet, 2006; Dunn and Hanchet, 2007). The same relationship has been used for both males and females. The present study indicates that the age of 50% spawning occurs at a much older age for females (16.6 years) on the Ross Sea slope and at (12.8 years) for males in the Ross Sea. The higher $A_{50\%}$ is a result of two factors. First, the original estimate of spawning at age 8 was based on studies of otolith banding patterns in a small number of unsexed fish (Burchett et al., 1984). A number of subsequent studies using GSI or histology have suggested a higher $A_{50\%}$ but did not provide a characterisation of oogenesis to enable a robust interpretation of the results (Patchell, 2001; Hanchet and Horn, 2000; Livingston and Grimes, 2005). Second, previous histological analyses have included fish with oocytes in the initial primary growth phase (CA stage) as developing to spawn in the upcoming season. Evidence from other notothenioids, from the characterisation of oogenesis presented here, and from histological hindcasting indicates that fish at the CA stage in summer months are at least a year away from spawning and should not be considered spawning. Hindcasting, which does not use the developmental stage of advancing oocytes to assign spawning status, provides a similar ogive to a forecasting method if fish advanced to at least the EVG stage are considered spawning. These fish should not be considered mature in the proportion spawning relationship. This issue, of characterising sexual development (which occurs only once) versus spawning (which may or may not occur each subsequent year) is detailed by Kock and Kellermann (1991) with specific application to fisheries management.

The spawning ogive represents the proportion of fish-at-age (or length) that will spawn in a typical year. For females, a percentage of sexually mature individuals skip-spawning each year. The proportion skipping appears to be age dependent, with more adolescent fish skipping than older fish (see Rideout et al., 2005; Jørgensen et al., 2006 for a theoretical discussion). The average annual spawning biomass is therefore decreased by the proportion of mature fish that do not spawn. This is the appropriate relationship to use to monitor spawning stock biomass (Kock and Kellermann, 1991; Constable et al., 2000; Murua et al., 2003).

Males may also skip spawning in theory (Jørgensen et al., 2006), but it is not apparent in the ogive with the limited samples available. Evidence from very low GSI levels of large males on the slope suggests that some sexually mature males may not maintain the typical residual GSI levels observed in northern areas and could skip. This may be related to the 'axe-handle' condition described by Fenaughty (2006), in which condition factors are exceptionally low due to severe loss of mass (both somatic and gonad). Comparing the ogives between males and females (forecasting ogive), on average females spawn more than four years later than males (Table 3). However, the difference is a result of three factors: (i) females generally begin developing when older; (ii) the female developmental process is longer; and (iii) skip-spawning flattens the female ogive resulting in a larger $A_{50\%}$.

All methods to determine age-at-spawning have some potential for bias. Figure 7 indicates that the hindcasting method actually detects slightly more adolescent spawning than the forecasting method. This is probably because forecasting using samples from early in the summer will not detect small fish that begin vitellogenesis later. The potential bias in hindcasting is that if remnant evidence of spawning from early fish is resorbed prior to sampling and early fish were a non-random subset of the population, the spawning ogive could be shifted. The analyses indicate this was not an issue as the proportion of fish at a given size containing POFs did not show a time trend.

Although the temporal dynamics associated with migration to the north for spawning are not fully understood, the estimated age distribution of spawning females on the slope matches the age distribution of all females observed in the northern area. This, combined with the lack of evidence of

skipped spawning in the north from histological samples, indicates that all the fish in the northern areas are spawning, and that the slope contains both fish developing to spawn for the first time, and recovering from spawning in previous seasons. It is not known if fish recovering from spawning on the slope had spawned in the north or spawned in some other location.

Because non-spawning fish do not appear to be present in the northern area, applying slope-derived ogives generates a bias in the estimation of spawning biomass that depends on the actual age structure in the northern area and the proportion of northern fish in the total population. Whether all fish in the north are indeed spawning remains to be confirmed. But if so, the larger the proportion of northern fish, and the younger the age structure of those fish, the more the overall population ogive would steepen and shift towards a younger age. Estimating the proportion of the population in the northern area will require spatially explicit population models (Dunn et al., 2009).

Antarctic fish typically mature to spawn when reaching 55–80% of maximum length (L_{max}) (Kock and Kellermann, 1991). For *D. mawsoni*, spawning at 133 cm equates to 66% of L_{max} (for females, 64% for males). However, one unique aspect of this late age-at-spawning is the relationship between natural mortality and age-at-spawning. Females spawn at an $A_{50\%}$ of 16 years, yet have a maximum age of approximately 35 years. If natural mortality on adult fish (estimated M = 0.13) occurs at a constant rate throughout the lifespan, then a relatively small proportion of females (~12.5%) reach the age at 50% spawning. This comparison is biased in that the $A_{50\%}$ at sexual maturity is likely lower by 1–2 years, but the proportion is still relatively low. This implies that spawning success must be high, which may be part of the selection pressure to produce large yolky eggs. Alternatively, it may imply that the natural mortality rate for this very large deep-sea species may be extremely low between settlement and spawning stages.

Conclusions

Although oogenesis has been well documented in studies of some notothenioid species during the past 40 years, integrating the peculiar developmental cycle with traditional methods of estimating age-at-spawning, and the constraints of sampling in summer months generated uncertainty in interpreting macroscopic, GSI and histological data for *D. mawsoni* males and females (Mormede et al., 2008).

Oogenesis in *D. mawsoni* closely follows the description provided by Shandikov and Faleeva (1992) for other notothenioids. The length-and age-at-spawning relationships presented here integrate the developmental cycle, large sample sizes and histological assessment to yield a consistent description of the reproductive life history for *D. mawsoni*. Details regarding the actual developmental timing for each cell stage transition, the time course of GSI development, breadth of the spawning season, fecundity, and egg buoyancy and spatial distribution are important life-history characteristics necessary to understanding the migratory cycle and require further investigation during the winter spawning season. That research and research to describe the functional role of males in the spawning strategy, to understand the factors driving skipped spawning, and to understand sex-specific migration behaviours will help to inform the development of spatially explicit population models (Dunn et al., 2009).

Acknowledgements

Thanks are due to the New Zealand Ministry of Fisheries science staff, scientific observers, and fishing crew who enabled and collected the data used for this analysis. G. Patchell generously provided histological slides from his previous work in the Ross Sea, greatly extending the seasonal range of samples available. The New Zealand Antarctic Fisheries Working Group provided helpful discussions and input into this paper. D. Ramm and E. Appleyard provided the data extracts from the CCAMLR Secretariat. We are grateful for the assistance of M. Carter, D. Fu and A. Wadhwa for graphics and histological work, S. Mormede for assistance with R code, and A. Dunn and S. Hanchet for stock assessment data and helpful discussions. We are especially grateful to D. Welsford and O. Kjesbu for their thoughtful reviews of an earlier draft. This project was funded by the New Zealand Ministry of Fisheries under project ANT2008/01.

References

Alekseyeva, Ye.I., F.Ye. Alekseyev, V.V. Konstantinov and V.A. Boronin. 1993. Reproductive biology of grenadiers, *Macrourus carinatus*, *M. whitsoni*, *Coelorinchus fasciatus* (Macrouridae), and *Patagonotothen guentheri shagensis* (Nototheniidae) and the distribution of *M. carinatus*. *J. Ichtyol.*, 33 (1): 71–84.

Burchett, M.S., A.L. DeVries and A.J. Briggs. 1984. Age determination and growth of *Dissostichus*

mawsoni (Norman, 1937) (Pisces, Nototheniidae) from McMurdo Sound (Antarctica). *Cybium*, 8 (1): 27–31.

Burton, M.P.M., R.M. Penney and S. Biddiscombe. 1997. Time course of gametogenesis in northwest Atlantic cod (*Gadus morhua*). *Can. J. Fish. Aquat. Sci.*, 54 (Suppl. S1): 122–131.

Constable, A.J., W.K. de la Mare, D.J. Agnew, I. Everson and D. Miller. 2000. Managing fisheries to conserve the Antarctic marine ecosystem: practical implementation of the Convention on the Conservation of Antarctic Marine Living Resources (CCAMLR). *ICES J. Mar. Sci.*, 57 (3): 778–791.

Dunn, A. and S.M. Hanchet. 2007. Assessment models for Antarctic toothfish (*Dissostichus mawsoni*) in the Ross Sea including data from the 2006/07 season. Document *WG-FSA-07/37*. CCAMLR, Hobart, Australia: 26 pp.

Dunn, A. and S.M. Hanchet. 2009. Assessment models for Antarctic toothfish (*Dissostichus mawsoni*) in the Ross Sea for the years 1997/98 to 2008/09. Document *WG-FSA-09/40 Rev. 1*. CCAMLR, Hobart, Australia: 31 pp.

Dunn, A., S. Rasmussen and S.M. Hanchet. 2009. Development of spatially explicit age-structured population dynamics operating models for Antarctic toothfish in the Ross Sea. Document *WG-SAM-09/18*. CCAMLR, Hobart, Australia: 44 pp.

Eastman, J.T. and A.L. DeVries. 2000. Aspects of body size and gonadal histology in the Antarctic toothfish, *Dissostichus mawsoni*, from McMurdo Sound, Antarctica. *Polar Biol.*, 23: 189–195.

Everson, I. 1970. Reproduction in *Notothenia neglecta* Nybelin. *Brit. Antarct. Surv. B.*, 23: 81–92.

Everson, I. 1984. Fish biology. In: Laws R.M. (Ed.). *Antarctic Ecology*, 2. Academic Press, London: 491–532.

Everson, I. 1994. Timescale of ovarian maturation in *Notothenia coriiceps*: evidence for a prolonged adolescent phase. *J. Fish Biol.*, 44: 997–1004.

Fenaughty, J.M. 2006. Geographical differences in the condition, reproductive development, sex ratio and length distribution of Antarctic toothfish (*Dissostichus mawsoni*) from the Ross Sea, Antarctica (CCAMLR Subarea 88.1). *CCAMLR Science*, 13: 27–45.

Hanchet, S.M. 2006. Species profile for Antarctic toothfish (*Dissostichus mawsoni*). Document *WG-FSA-06/26*. CCAMLR, Hobart, Australia: 22 pp.

Hanchet, S.M. and P.L. Horn. 2000. The Ross Sea Antarctic toothfish (*Dissostichus mawsoni*) fishery from 1997/98 to 1999/2000. Document *WG-FSA-00/55*. CCAMLR, Hobart, Australia: 31 pp.

Hanchet, S.M., G.J. Rickard, J.M. Fenaughty, A. Dunn and M.J. Williams. 2008. A hypothetical life cycle for Antarctic toothfish (*Dissostichus mawsoni*) in the Ross Sea region. *CCAMLR Science*, 15: 35–53.

Horn, P.L. 2002. Age and growth of Patagonian toothfish (*Dissostichus eleginoides*) and Antarctic toothfish (*D. mawsoni*) in waters from the New Zealand subantarctic to the Ross Sea, Antarctica. *Fish. Res.*, 56 (3): 275–287.

Jørgensen, C., B. Ernande, Ø. Fiksen and U. Dieckmann. 2006. The logic of skipped spawning in fish. *Can. J. Fish. Aquat. Sci.*, 63 (1): 200–211.

Junquera, S., E. Román, J. Morgan, M. Sainza and G. Ramilo. 2003. Time scale of ovarian maturation in Greenland halibut (*Reinhardtius hippoglossoides*, Walbaum). *ICES J. Mar. Sci.*, 60 (4): 767–773.

Kock, K.-H. and A. Kellermann. 1991. Review. Reproduction in Antarctic notothenioid fish. *Ant. Sci.*, 3 (2): 125–150.

Livingston, M.E. and P.J. Grimes. 2005. Size at maturity and histological procedures explored to determine spawning activity of female *Dissostichus mawsoni* from sample collected in the Ross Sea in January 2004, December 2004 and January 2005. Document *WG-FSA-05/63*. CCAMLR, Hobart, Australia.

Mormede, S., S.J. Parker and P. Grimes. 2008. Investigating length at maturity of Antarctic toothfish (*Dissostichus mawsoni*) based on scientific observers' data. Document *WG-FSA-08/48*. CCAMLR, Hobart, Australia: 26 pp.

Murua, H., G. Kraus, F. Saborido-Rey, P.R. Witthames, A. Thorsen and S. Junquera. 2003. Procedures to estimate fecundity of marine fish species in relation to their reproductive strategy. *J. Northw. Atl. Fish. Sci.*, 33: 33–54.

Patchell, G. 1999. Problems with estimation of size at maturity of *Dissostichus mawsoni* in Subarea 88.1. Document *WG-FSA-99/74*. CCAMLR, Hobart, Australia: 7 pp.

Patchell, G. 2001. Information on the spawning season and size of maturity of *Dissostichus mawsoni* from Subarea 88.1 in the 2000/01 season. Document *WG-FSA-01/51*. CCAMLR, Hobart, Australia: 10 pp.

Piyanova, S.V. 2008. Some data on the reproductive system condition of Antarctic toothfish (*Dissostichus mawsoni*) males and females from the Indian Ocean area in summer. ICES CM 2008/C:09: 11 pp.

Piyanova, S.V. and A.F. Petrov. 2007. The oogenesis characteristics of Antarctic toothfish *Dissostichus mawsoni Norman* 1937 (Perciformes Nototheniidae) caught by the bottom longline in the Ross Sea. PICES/ICES Conference 'New Frontiers in Marine Science', 26 to 29 June 2007, Baltimore, MD, USA: 24 pp.

Rideout, R.M., G.A. Rose and M.P.M. Burton. 2005. Skipped spawning in female iteroparous fishes. *Fish Fish.*, 6 (1): 50–72.

Saborido-Rey, F. and S. Junquera. 1998. Histological assessment of variations in sexual maturity of cod (*Gadus morhua* L.) at the Flemish Cap (northwest Atlantic). *ICES J. Mar. Sci.*, 55 (3): 515–521.

Shandikov, G.A. and T.I. Faleeva. 1992. Features of gametogenesis and sexual cycles of six notothenioid fishes from East Antarctica. *Polar Biol.*, 11 (8): 615–621.

Sil'yanova, Z.S. 1982. Oogenesis and stages of maturity of fishes of the family Nototheniidae. *Voprosy Ichthiologii*, 21 (4): 687–694. Translated as *J. Ichthyol.*, 21 (4): 81–89.

West, G. 1990. Methods of assessing ovarian development in fishes: a review. *Aust. J. Mar. Freshw. Res.*, 41: 199–222.

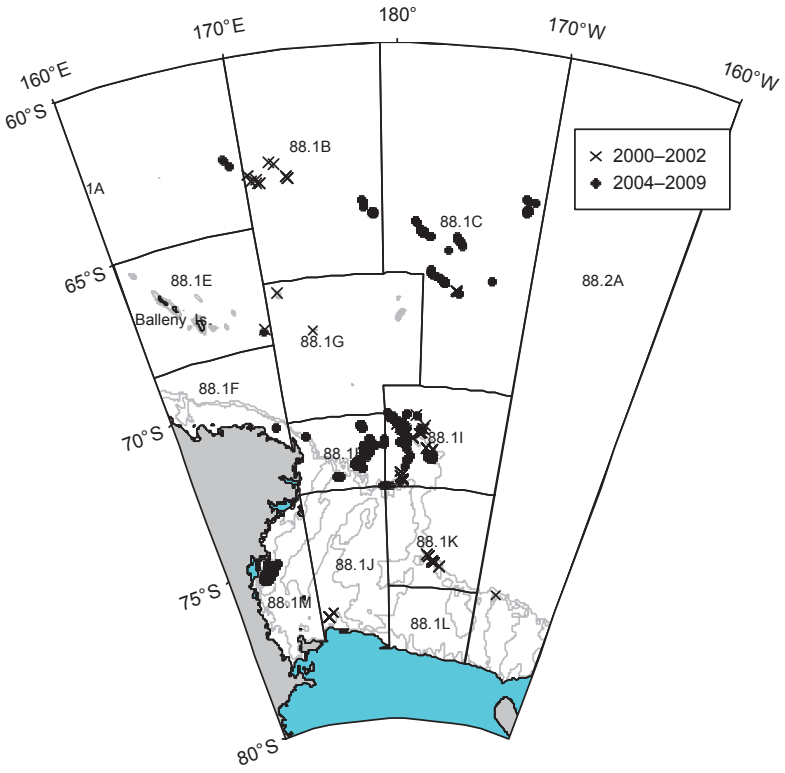

Figure 1: CCAMLR Subarea 88.1 and SSRU 882A indicating locations of gonad sample collections from *Dissostichus mawsoni* from 2000 to 2009 from small-scale research units (SSRUs) in the northern (SSRUs 881A, B, C, G), shelf (SSRUs 881J, M) and slope (SSRUs 881H, I, K) regions. Bathymetry contours at 500, 1 000 and 1 500 m are indicated by grey lines.

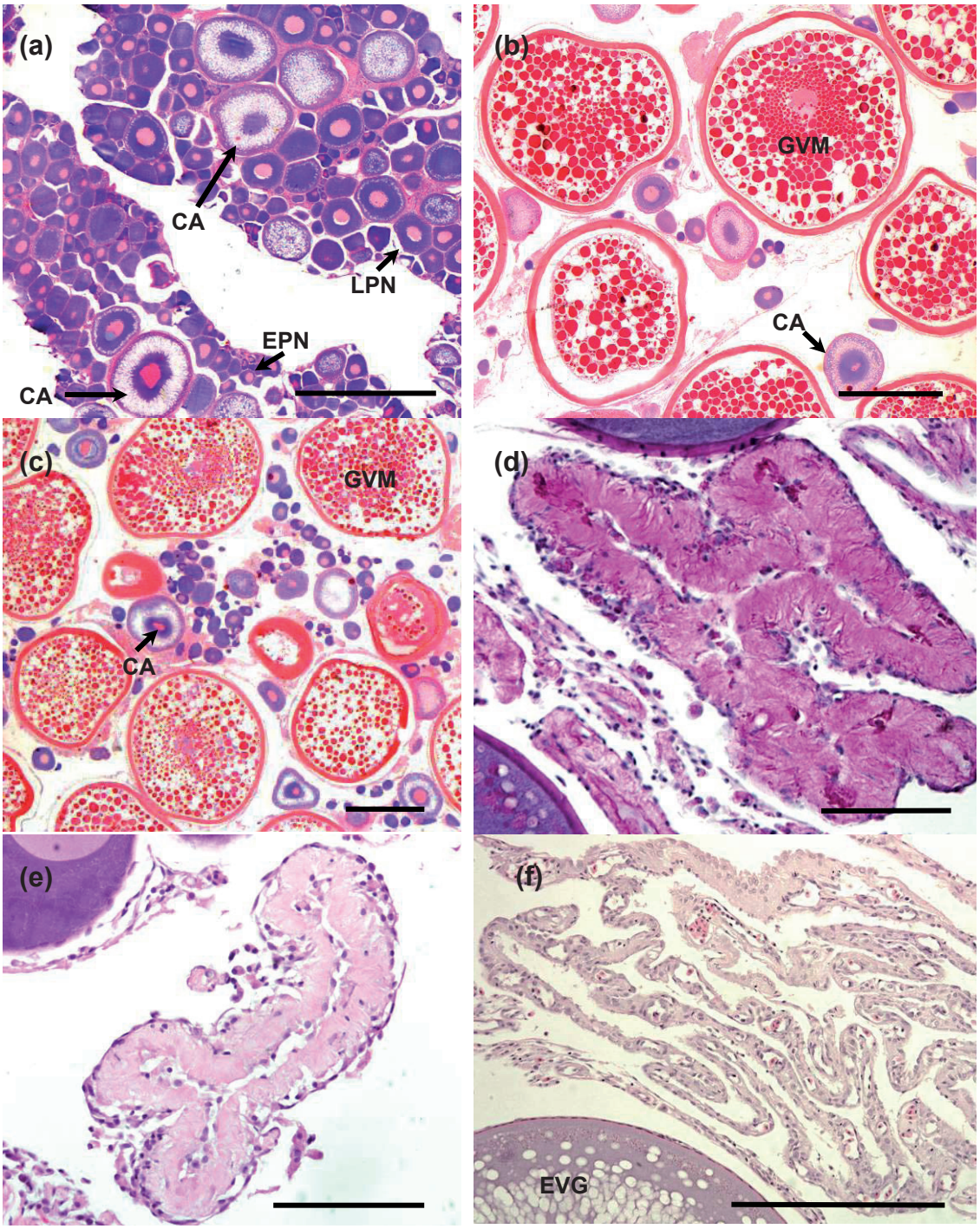

Figure 2: Examples of ovarian sections from *Dissostichus mawsoni* developing oocytes (a–c) and post-ovulatory follicles (d–f) present up to seven months after a hypothesised July spawning date. Fish lengths were (a) 107 cm, (b) 144 cm, (c) 164 cm, (d) 139 cm, (e) 153 cm, and (f) 159 cm. (a–c) have scale bar 1 000 µm and Periodic acid-Schiff (PAS) stain, (d–f) have scale bar of 100 µm and Haematoxylin and Eosin (H&E) stain. EPN – early perinucleolus, LPN – late perinucleolus, CA – cortical alveoli, EVG – early vitellogenesis, GVM – germinal vesicle migration. Photos by NIWA.

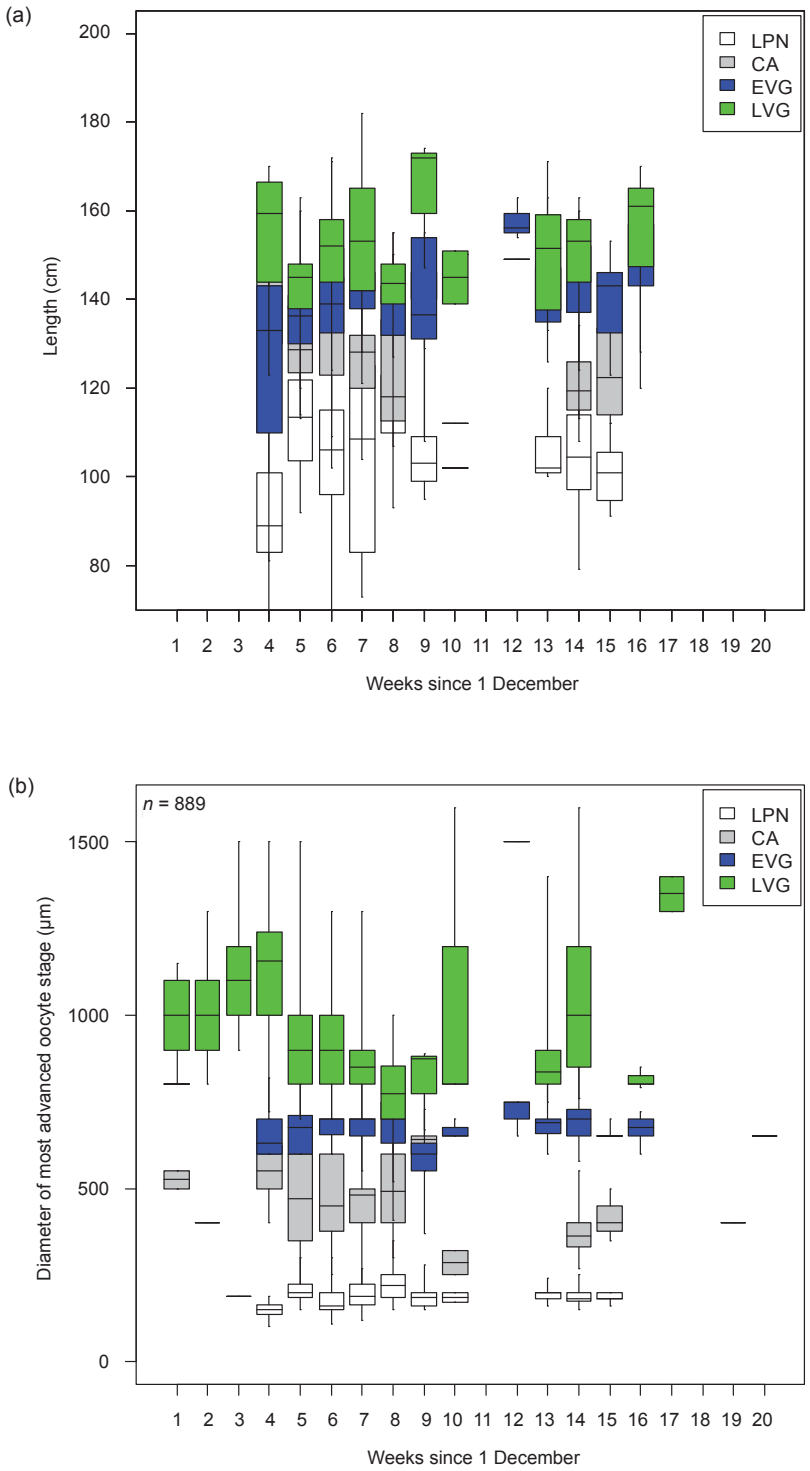

Figure 3: (a) Boxplot of fish length distributions in the slope area for individuals at each histological stage by week for *Dissostichus mawsoni* sampled in the Ross Sea, 2000–2009. (b) Boxplot of oocyte diameters for fish at each developmental stage from histological preparations summarised by week. Horizontal lines indicate the median size, boxes indicate the inter-quartile range and vertical lines indicate the range. LPN – late perinucleolus, CA – cortical alveoli, EVG – early vitellogenesis, LVG – late vitellogenesis.

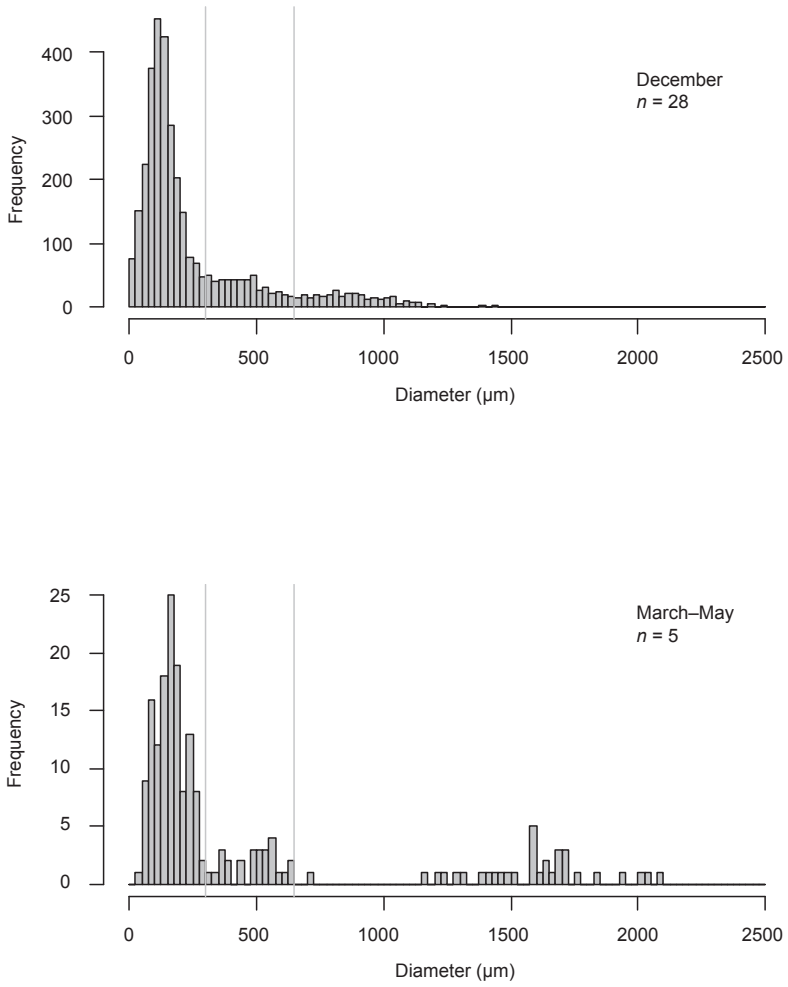

Figure 4: Composite oocyte size distribution for developing fish in December (upper panel) compared with the distribution in late March–May (lower panel) showing the growth and separation of the developing size mode of oocytes. Vertical lines indicate the approximate size range of oocytes at the cortical alveoli stage. Note: counts are of oocytes visible in the slide section. Very small oocytes and cells within oogonial nests are under-represented in the histograms.

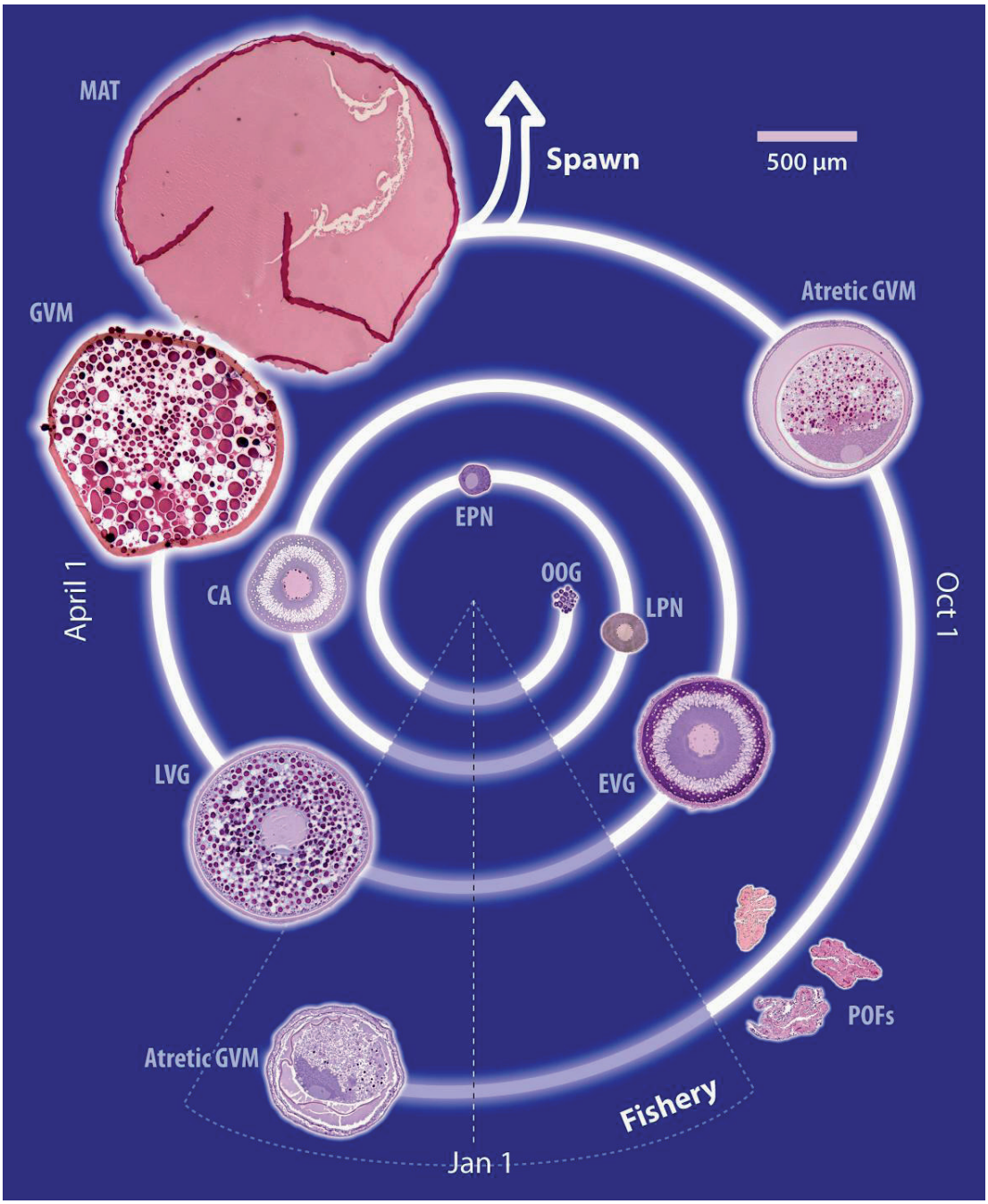

Figure 5: Diagrammatic representation of oogenesis in *Dissostichus mawsoni*. The process is represented by a calendar, with the oocyte states present in an ovary in a given month represented by a cross-section from the figure's centre to the outside edge. The first year represents initial generation of oocytes through perinucleolus stage. This is followed by a year (or more) of growth at the cortical alveoli stage. A final year of vitellogenesis and spawning completes a two-year developmental process, with cell and follicle remnants present afterwards. Photograph insets show examples of cells at each stage, scaled relative to each other. Maximum cell size depicted is 2 500 µm. Variations in this process are mainly through individuals being slightly advanced or delayed compared to the average. OOG – oogonia, EPN – early perinucleolus, LPN – late perinucleolus, CA – cortical alveoli, EVG – early vitellogenesis, LVG – late vitellogenesis, GVM – germinal vesicle migration, MAT – maturing, POFs – post-ovulatory follicles. Note that to obtain true relative scale of cell size, the GVM and the MAT cell sizes would need to be inflated by another 30%.

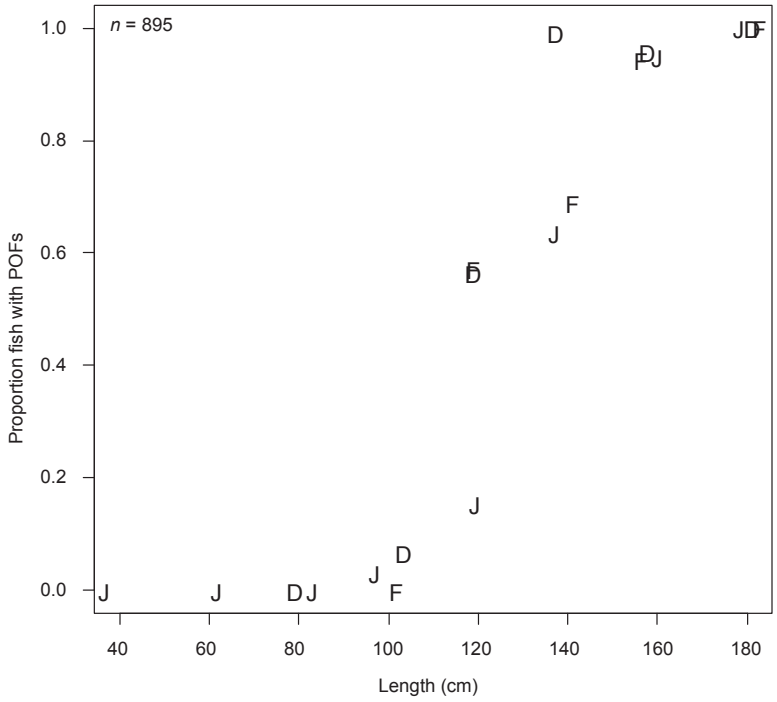

Figure 6: Proportion of fish showing post-ovulatory follicles by fish size (arranged in 20 cm bins) for December (D), January (J) and February (F). Symbols are slightly jittered horizontally for readability.

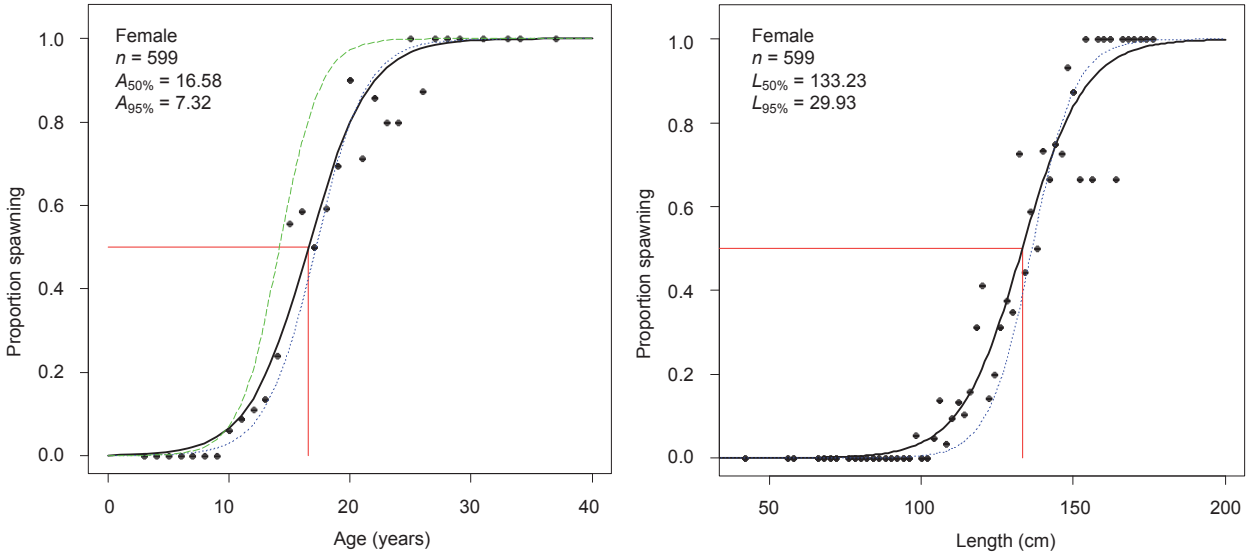

Figure 7: Plot of the spawning ogives for female *Dissostichus mawsoni* sampled on the Ross Sea slope. Points and the thick black line show hindcasting ogive. A blue dashed line shows the fit using forecasting data. The green long dashed line shows the proportion of fish reaching at least the cortical alveoli stage (termed the CA stage ogive in text). Red lines indicate the $A_{50\%}$ or $L_{50\%}$ for the hindcast ogive.

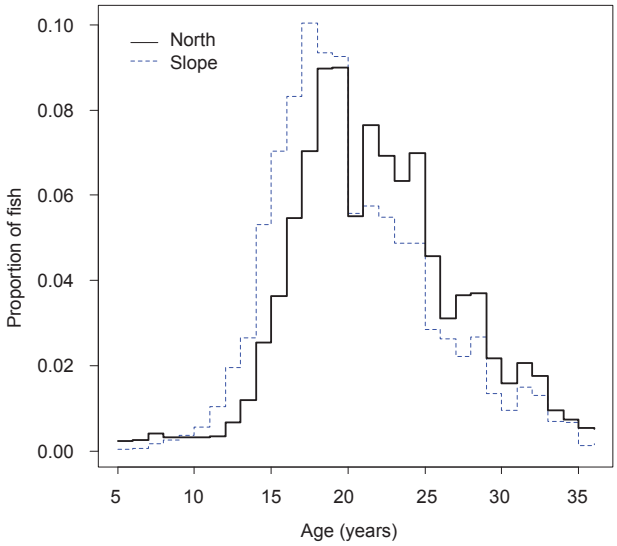

Figure 8: Histograms of the scaled age-frequency distribution of all northern females compared with the scaled age-frequency distribution of spawning-only females from the slope.

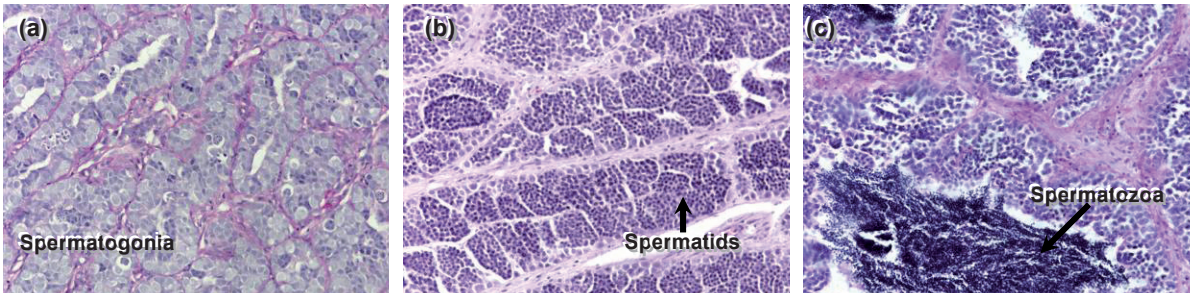

Figure 9: Testes at different stages of development: (a) immature with spermatogonia and some early spermatocytes; (b) developing with spermatogonia, spermatocytes and spermatids; (c) spawning with spermatozoa filling the lobular space. Sections were PAS stained and images taken at x200 magnification.

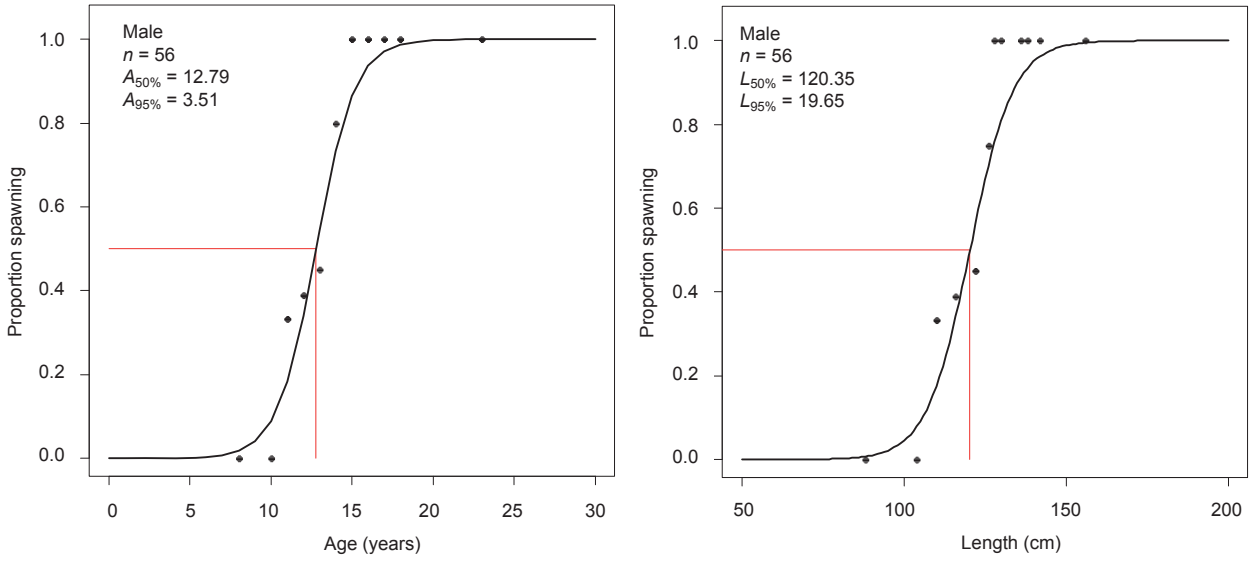

Figure 10: Age- and length-at-spawning ogives for male *Dissostichus mawsoni* from the Ross Sea. Red lines indicate the $A_{50\%}$ or $L_{50\%}$.

Liste des tableaux

Liste des figures

Figure 6: Proportion de poissons présentant des follicules post-ovulatoires en fonction de la taille des poissons (regroupés en lots de 20 cm) en décembre (D), janvier (J) et février (F). Les symboles sont légèrement décalés sur le plan horizontal pour faciliter la lecture.

Figure 7: Graphique des ogives de reproduction des femelles de *Dissostichus mawsoni* échantillonnées sur la pente de la mer de Ross. Les points et la ligne noire épaisse montrent l'ogive de rétrodiction. Une ligne bleue tiretée montre l'ajustement aux données de prédiction. La ligne verte en tirets longs montre la proportion de poissons ayant atteint au moins le stade des alvéoles corticaux (mentionné sous le terme "CA stage ogive" dans le texte). Les lignes rouges indiquent $A_{50\%}$ ou $L_{50\%}$ de l'ogive de rétrodiction.

Figure 8: Histogrammes de la distribution étalonnée de fréquences d'âges de toutes les femelles du nord comparés à ceux de la distribution étalonnée de fréquences d'âges des femelles reproductrices de la pente.

Figure 9: Testicules à des différents stades de développement : (a) immatures avec des spermatogones et quelques spermatocytes précoces ; (b) en voie de développement avec des spermatogones, spermatocytes et spermatides ; (c) en voie de reproduction avec des spermatozoïdes remplissant l'espace lobulaire. Les coupes ont été teintées par le colorant PAS et le grossissement des clichés est de x 200.

Figure 10: Ogives de longueur ou d'âge à la reproduction de *Dissostichus mawsoni* mâles de la mer de Ross. Les traits rouges indiquent $A_{50\%}$ ou $L_{50\%}$.

Список таблиц

Табл. 1: Временное и пространственное распределение образцов яичников *Dissostichus mawsoni*, собранных научными наблюдателями в ходе ярусного промысла в море Росса. Примечание: только образцы, полученные в период с декабря по март в районе склона, использовались для определения огивы доли нерестящихся самок. Образцы, полученные в другие периоды и в других районах, использовались для описания цикла развития.

Табл. 2: Сводные данные о стадиях развития в соответствии с гистологической оценкой яичников *Dissostichus mawsoni*, собранных в летние промысловые месяцы в море Росса, 2004–2009 гг. Цифры – количество особей рыбы. EPN – ранние перинуклеолы, LPN – поздние перинуклеолы, CA – кортикальные альвеолы, EVG – ранний вителлогенез, LVG – поздний вителлогенез, GVM – миграция зародышевых пузырьков, MAT – созревание.

Табл. 3: Информация о подобранных огивах для длины или возраста при нересте *Dissostichus mawsoni* в море Росса с использованием методов ретроспективного и перспективного прогноза. $L_{95\%}$ или $A_{95\%}$ означают длину или возраст, которые следует добавить к значению $L_{50\%}$, чтобы получить 95-ю процентиль.

Список рисунков

Рис. 1: Подрайон 88.1 и SSRU 882A АНТКОМ, с указанием мест сбора образцов гонад *Dissostichus mawsoni* в период 2000–2009 гг. из мелкомасштабных исследовательских единиц (SSRU) в районах севера (SSRU 881A, B, C, G), шельфа (SSRU 881J, M) и склона (SSRU 881H, I, K). Изобаты 500, 1 000 и 1 500 м показаны серыми линиями.

Рис. 2: Примеры овариальных срезов развивающихся ооцитов (a–c) и постовуляционных фолликул (d–f) *Dissostichus mawsoni* , присутствующие вплоть до семи месяцев после предполагаемой даты нереста в июле.Длина особей составляла: (a) 107 см, (b) 144 см, (c) 164 см, (d) 139 см, (e) 153 см и (f) 159 см. (a–c) имеют масштабную метку, равную 1 000 μм, и окрашены реактивом Шиффа (PAS), (d–f) имеют масштабную метку, равную 100 μм, и окрашены гематоксилином и эозином (H&E). (EPN – ранние перинуклеолы, LPN – поздние перинуклеолы, CA – кортикальные альвеолы, EVG – ранний вителлогенез, GVM – миграция зародышевых пузырьков). Фотография сделана NIWA.

Рис. 3: (a) Коробчатая диаграмма распределений длин рыбы в районе склона для особей на каждой гистологической стадии по неделям для образцов *Dissostichus mawsoni*, полученных в море Росса, 2000–2009 гг. (b) Коробчатая диаграмма обобщенных по неделям диаметров ооцитов для рыбы на каждой стадии развития по гистологическим препаратам.Горизонтальные линии показывают

медианный размер, ящички – интерквартильный размах, а вертикальные линии – диапазон. LPN – поздние перинуклеолы, CA – кортикальные альвеолы, EVG – ранний вителлогенез, LVG – поздний вителлогенез.

Рис. 4: Составное распределение размеров ооцитов у развивающейся рыбы в декабре (верхний график) в сравнении с распределением в конце марта–мае (нижний график), где показан рост и разделение развивающейся размерной моды ооцитов. Вертикальные линии показывают приблизительный размерный диапазон ооцитов на стадии кортикальных альвеол. Примечание: подсчитываются ооциты, видимые на срезе. На гистограммах представлено мало очень мелких ооцитов и клеток в группах оогоний.

Рис. 5: Схематическое изображение оогенеза у *Dissostichus mawsoni*. Процесс представлен в соответствии с календарем; состояние ооцитов, имеющихся в яичниках в указанный месяц, представлено разрезом от центра рисунка к внешнему краю. Первый год представляет первоначальное формирование ооцитов на стадии перинуклеол. Затем следует год (или более) роста на стадии кортикальных альвеол. Последний год вителлогенеза и нерест завершают двухлетний процесс развития; остатки клеток и фолликул имеются и после этого. На фото вставках показаны образцы клеток на каждой стадии, масштабированные по отношению друг к другу. Максимальный представленный размер клетки – 2 500 μм. Отклонения в данном процессе в основном обусловлены тем, что отдельные особи могут быть несколько более развитыми или отставать в развитии по сравнению со средним. OOG – оогония, EPN – ранние перинуклеолы, LPN – поздние перинуклеолы, CA – кортикальные альвеолы, EVG – ранний вителлогенез, LVG – поздний вителлогенез, GVM – миграция зародышевых пузырьков, MAT – созревание, POF – постовуляторные фолликулы. Примечание: для получения действительного относительного масштаба размеров клеток потребовалось бы увеличить размеры клеток GVM и MAT еще на 30%.

Рис. 6: Доля рыбы, имеющей постовуляторные фолликулы, в соответствии с размерами рыбы (показаны с интервалами 20 см) в декабре (D), январе (J) и феврале (F). Знаки несколько разбросаны по горизонтали с целью удобочитаемости.

Рис. 7: График нерестовых огив самок *Dissostichus mawsoni*, отобранных на склоне моря Росса. Точки и жирная черная линия показывают ретроспективную огиву. Синяя пунктирная линия показывает подбор с использованием данных прогноза. Зеленая прерывистая линия показывает долю рыбы, достигшей по крайней мере стадии кортикальных альвеол (в тексте называется "огива на стадии CA). Красные линии показывают $A_{50\%}$ или $L_{50\%}$ для ретроспективной огивы.

Рис. 8: Гистограммы пересчитанного распределения частоты возрастов всех северных самок по сравнению с пересчитанным распределением частоты возрастов только нерестовых самок на склоне.

Рис. 9: Семенники на разных стадиях развития: (a) незрелые со сперматогониями и некоторым количеством ранних сперматоцитов; (b) развивающиеся со сперматогониями, сперматоцитами и сперматидами; (c) нерестовые со сперматозоидами, заполнившими лобулярное пространство. Срезы были окрашены PAS и снимки сделаны с увеличением x200.

Рис. 10: Огивы возраста и длины при нересте для самцов *Dissostichus mawsoni* из моря Росса. Красные линии показывают $A_{50\%}$ или $L_{50\%}$.

Lista de las tablas

Tabla 1: Distribución temporal y espacial de las muestras de ovarios de *Dissostichus mawsoni* recogidas por observadores científicos en las pesquerías de palangre en el Mar de Ross. Nótese que sólo se utilizaron las muestras tomadas de diciembre a marzo en la región del talud para determinar la ojiva de la proporción de hembras desovantes. Se utilizaron muestras de otras épocas y lugares para describir el ciclo de desarrollo.

Tabla 2: Resumen del estadio de desarrollo sobre la base del examen de muestras histológicas de ovarios de *Dissostichus mawsoni* recogidas durante los meses de pesca en verano en el Mar de Ross, 2004–2009. Los valores representan el número de peces. EPN – fase perinucleolar inicial, LPN – faseperinucleolar tardía, CA – alvéolo cortical, EVG – vitelogénesis inicial, LVG – vitelogénesis tardía, GVM – migración de la vesícula germinal, MAT – maduración.

Tabla 3: Detalles de los ajustes de la ojiva de talla o edad de desove para *Dissostichus mawsoni* del Mar de Ross mediante metodologías que interpretan los resultados hacia atrás (*hindcasting*) o hacia delante (*forecasting*) en el tiempo. Bajo la columna $L_{95\%}$ o $A_{95\%}$ se indica la longitud o la edad que debe agregarse al valor de $L_{50\%}$ para alcanzar el percentil 95.

Lista de las figuras

Figura 1: Mapa de la Subárea 88.1 de la CCRVMA y de la UIPE 882A donde se indican los lugares de donde provienen las muestras de gónadas de *Dissostichus mawsoni* de 2000 a 2009 capturados dentro de las unidades de investigación en pequeña escala (UIPE) en la zona norte (UIPE 881A, B, C, G), en la plataforma (UIPE 881J, M) y en el talud (UIPE 881H, I, K). Los contornos batimétricos de 500, 1 000 y 1 500 m se han trazado en líneas grises.

Figura 2: Ejemplos de secciones histológicas de ovario de *Dissostichus mawsoni* con ovocitos en crecimiento (a–c) y folículos post-ovulatorios (d–f) presentes hasta siete meses después de una fecha de desove hipotética en julio. Las tallas de los peces fueron (a) 107 cm, (b) 144 cm, (c) 164 cm, (d) 139 cm, (e) 153 cm y (f) 159 cm. Muestras (a–c) a escala de 1 000 μm y tinción con ácido periódico de Schiff (PAS); (d–f) tienen escala de 100 μm y tinción hematoxilina-eosina (H&E). (EPN – fase perinucleolar inicial, LPN – fase perinucleolar tardía, CA – alvéolo cortical, EVG – vitelogénesis inicial, GVM – migración en la vesícula germinal. Fotografías de NIWA.

Figura 3: (a) Diagrama de cajas de la distribución por tallas de *Dissostichus mawsoni* en el área del talud para los especímenes recolectados en el Mar de Ross (2000–2009) por etapa histológica semanal. (b) Diagrama de cajas del diámetro de ovocitos en cada estadio de desarrollo de los peces, de preparaciones histológicas resumidas por semana. Las líneas horizontales indican el tamaño mediano, las cajas muestran el rango intercuartílico y las líneas verticales muestran el rango. LPN – fase perinucleolar tardía, CA – alvéolo cortical, EVG – vitelogénesis inicial, LVG – vitelogénesis tardía.

Figura 4: Distribución compuesta del tamaño de los ovocitos de los peces en desarrollo en diciembre (panel superior), comparado con la distribución a fines de marzo-mayo (panel inferior); se muestra el crecimiento y desfase en el crecimiento de los ovocitos. Las líneas verticales indican el rango aproximado del tamaño de los ovocitos en la fase de alvéolo cortical. Nota: se han contado los ovocitos visibles en el corte histológico sobre el portaobjeto. Los ovocitos y células muy pequeños dentro de los nidos de ovogonias están representados por lo bajo en los histogramas.

Figura 5: Diagrama de la ovogénesis en *Dissostichus mawsoni*. El proceso está representado por un calendario, con muestras de los estadios de desarrollo de ovocitos en el ovario en un mes dado, desde el centro de la figura hasta la periferia. El primer año representa la generación inicial de ovocitos hasta el estado perinucleolar. Esto es seguido de un año (o más) de crecimiento en la fase de alvéolo cortical. Un año final de vitelogénesis y desove completa un proceso de desarrollo de dos años, apareciendo posteriormente restos de células y folículos. Las fotografías muestran ejemplos de células en cada etapa, siendo el tamaño proporcional entre sí. El tamaño máximo de la célula mostrado es de 2 500 μm. Las variaciones en este proceso ocurren principalmente por la diferencia individual en el desarrollo, es decir, están levemente más avanzados o rezagados en comparación con el promedio. OOG – ovogonia, EPN – fase perinucleolar inicial, LPN – fase perinucleolar tardía, CA – alvéolo cortical, EVG – vitelogénesis inicial, LVG – vitelogénesis tardía, GVM – migración dentro de la vesícula germinal, MAT – maduración, POFs – folículos post-ovulatorios. Nótese que para obtener el tamaño real de la célula a escala, el tamaño de las células GVM y MAT tendrían que aumentarse 30%.

Figura 6: Proporción de peces con folículos post-ovulatorios por talla (por intervalo de 20 cm) en diciembre (D), enero (J) y febrero (F). Los símbolos se han corrido levemente para facilitar su lectura.

Figura 7: Ojivas de desove para las hembras de *Dissostichus mawsoni* de la zona del talud del Mar de Ross. Los puntos y la línea gruesa negra muestran la ojiva derivada de los datos existentes. La línea entrecortada en azul muestra el ajuste usando los datos extrapolados. La línea entrecortada más grande de color verde muestra la proporción de peces que alcanzan por lo menos el estadio de alvéolo cortical (denominado ojiva en estadio CA en el texto). Las líneas rojas muestran $A_{50\%}$ o $L_{50\%}$ para la ojiva en el pasado.

Figura 8: Histogramas de la distribución a escala de las frecuencias de edades de todas las hembras del norte y la distribución a escala de las frecuencias de edades de las hembras desovantes solamente en la zona del talud.

Figura 9: Testículos en distintos estadios de desarrollo (a) inmaduros con espermatogonia y algunos espermatocitos tempranos; (b) en desarrollo con espermatogonia, espermatocitos y espermátidas; (c) en desove con espermatozoides llenando el espacio lobular. Secciones teñidas con PAS y magnificación de las imágenes x200.

Figura 10: Ojivas de la edad y de la talla de espermiación de los machos de *Dissostichus mawsoni* capturados en el Mar de Ross. Las líneas rojas muestran $A_{50\%}$ o $L_{50\%}$.